Design procedure for pot-core integrated magnetic component

Martin Foster, Department of Electronic and Electrical Engineering, University of Sheffield, Mappin Street, Sheffield, United Kingdom, m.p.foster@sheffield.ac.uk

Andrew Fairweather & Grant Ashley, VxI Power Ltd, Station Rd, North Hykeham, Lincoln, LN6 3QY, United Kingdom, andrew.fairweather@vxipower.com, grant.ashley@vxipower.com

Abstract

The side-by-side (primary-secondary) wound integrated magnetic component is often used to combine series inductance and transformer behaviour in LLC resonant converters and dual active bridge converters. This paper presents an easy to follow design procedure for this component, translating the component's electrical specification into a physical design. A combination of reluctance modelling, the application of Ampere's law and the introduction of an alignment factor, obtained through finite element analysis, is used to derive a model for the integrated magnetic component. The model is encapsulated within a design approach accounting for frequency, maximum operating flux density, etc., to ensure the final component is not oversized and meets the design specification.

1. Introduction

Design aesthetics, volume constraints, efficiency improvements, cost and the drive towards tighter system integration pose significant challenges for the power supply engineer, who often finds these drivers are in direct conflict with thermal and packaging constraints. In order to meet these ever increasing demands, the main inductor and transformer of the power converter are often combined into a single integrated magnetic (IM) component in an effort to save volume and cost. The transition to IM has led to the proliferation of modern power supply circuits, such as the LLC resonant converter and the dual active bridge, where the presence of transformer series and magnetizing inductances are readily absorbed into the circuit and provide useful functions, such as current provision for soft-switching. Many integrated magnetic components have been proposed, eg. using a shared primary winding with separate cores to realise both inductance and transformer [1]; placing various windings on the different legs of an E-core structure to construct inductors and transformers [2]; physically separating the primary and secondary windings, side-by-side on the core's centre leg to introduce leakage inductance between the two windings [3]. The side-by-side winding format is particularly attractive as the spacing between the windings can be used to meet the necessary creepage and clearance requirements, and provides the particular focus for this paper.

Traditionally, magnetic equivalent circuit techniques have been employed to model IM components. For certain IM structures magnetic equivalent circuits work very well where the core structure leads to logical partitioning in the equivalent circuit [1,2]. However, for the side-by-side IM structure equivalent circuit modelling leads to inaccurate estimation of the leakage due to the lack of granularity in representing the magnetic field strength distribution. Although a distributed mmf-reluctance model can be employed, where the winding mmf source and coil winding area reluctance contributions are evenly divided over the region of interest [4], the technique is somewhat unwieldy and the developed equivalent circuit model is cumbersome. Therefore, it does not readily lend itself to application in design. A more successful alternative is to equate the energy stored in the IM leakage inductances to energy stored in the winding volume by applying Ampere's law [5]. Although this technique was applied to the side-by-side IM in [3], the application of the resulting model is obfuscated by the various transformer equivalent circuit models described in the manuscript and the

numerous definitions for the transformer coupling factor. This paper derives a completely new model based on a combination of reluctance modelling, application of Ampere's law and an alignment factor obtained through finite element modelling. The resulting model is easy to apply and is encapsulated within a design procedure.
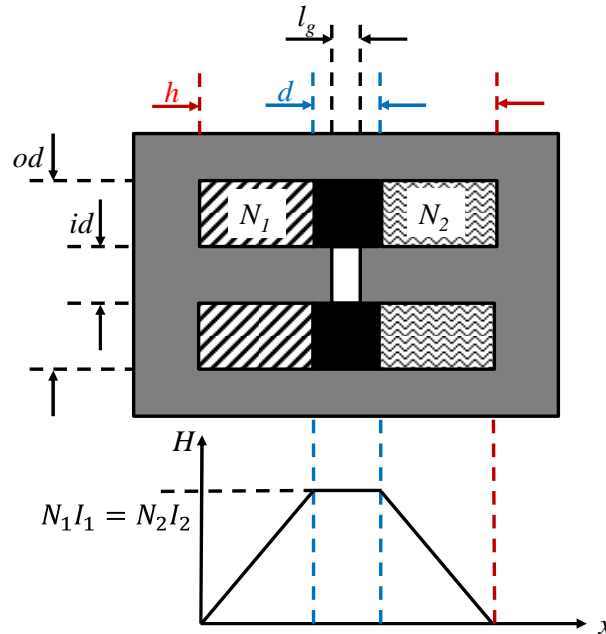
Fig. 1. Integrated magnetic component, geometry and magnetic field intensity

2. Transformer equivalent circuit

The transformer equivalent circuit in Fig. 2 captures the dominant behavior of a transformer using just four components: a primary-side series inductor (L_{lk1}), to model the leakage inductance present on the primary side of the transformer, a shunt inductor (L_m), to model the magnetizing inductance, an ideal transformer with a turn ratio (n_e) and a secondary-side series inductor (L_{lk2}).
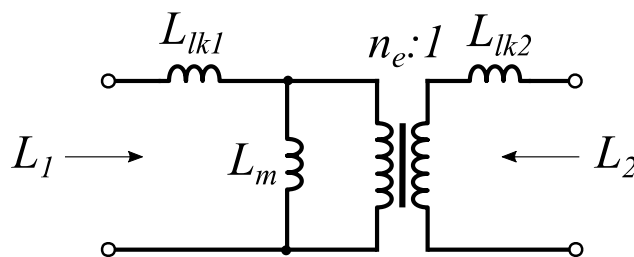
Fig. 2. Transformer equivalent circuit

2.1.   Measuring transformer equivalent circuit values

Inductors L_1 and L_2 represent the transformer's primary winding inductance (measured using terminals A & B) and secondary winding inductance (measured using terminals C & D), respectively. The inductance values of both windings can be measured with the other winding connected as an open-circuit (oc) or short-circuit (sc). Using these types of measurements allows the parameters for the equivalent circuit to be found as follows:

- $L_{lk1}+L_m=L_{1(oc)}$: L_1 is measured with the secondary winding open circuit
- $L_{lk1}+L_m||n_e^2L_{lk2}=L_{1(sc)}$: L_1 is measured with the secondary winding short circuit
- Actual turn ratio $n=N_1/N_2\approx\sqrt{(L_{1(oc)}/L_{2(oc)})}$ where N_1 and N_2 are the primary and secondary winding turns, respectively
- M: The mutual inductance coupling the primary winding to the secondary winding can be found using $M=\sqrt{((L_{1(oc)}-L_{1(sc)})L_{2(oc)})}$
- k: Coupling coefficient $k=M/\sqrt{(L_{1(oc)}\ L_{2(oc)})}$
- $L_m=k^2L_{1(oc)}$
- $L_{lk1}=(1-k^2)L_{1(oc)}$
- n_e: *equivalent turn ratio* $n_e\approx\sqrt{(L_m/L_{2(oc)})}$ – assuming L_{lk2} is negligible

2. Pot-core integrated magnetic component

The objective of this section is to derive a mathematical model to predict the leakage inductance of the IM. Fig. 2 shows a cross section through the centre of the pot-core integrated magnetic component revealing a primary winding of N_1 turns and a secondary winding of N_2 turns. An airgap of length l_g is used to control inductance. It is assumed the primary and secondary windings are wound on a bobbin with an outer diameter od, inner diameter id, height h and with a separator of length d located between the two windings. The plot below the IM cross section shows how the magnetic field intensity H varies across the height the bobbin moving in the x direction.

The inductance for primary winding and the secondary winding with the secondary winding open circuit is,

$$L_{1(oc)} = A_L N_1{}^2 (AF) \tag{1}$$

where A_L is the core specific inductance. AF is an alignment factor that accounts for the effects of coil winding height and its location within the winding window and is described in section 3.
The secondary winding inductance is similarly defined as

$$L_{2(oc)} = A_L N_2{}^2 (AF) \tag{2}$$

The energy stored in the leakage inductance due to the peak primary current $I_{1(pk)}$ is given by

$$W_{Llk1} = 0.5 L_{lk1} I_{1(pk)}{}^2 \tag{3}$$

If the permeability of the core is very much higher than that of the coil windings, then it can be assumed that this energy is stored in the winding and so it can be determined from the volume integral of the BH product,

$$W_{Llk1} = \frac{1}{2}\int BH dv = \frac{\mu_0}{2}\int H^2 dv = \frac{\mu_0}{2}\int\int\int H(r,\theta,x)^2 r dr d\theta dx \tag{4}$$

Since the winding can be considered to be a tube, (4) is evaluated over the volume of winding tube. The magnetic field intensity at a specific height (x) in the tube is assumed to be approximately constant across the winding width, $w=0.5(od-id)$, such that,

$$H = \frac{x}{a}\frac{N_1 I_{1(pk)}}{w} \tag{5}$$

for $0<x<a$ where $a=(h-d)/2$.

The contribution from N_1 can be found by using (5) to evaluate (4) as follows,

$$W_{Llk1(N1)} = \frac{\mu_0}{2}\int_{r1}^{r2}\int_0^{2\pi}\int_0^a \left(\frac{x}{a}\frac{N_1 I_{1(pk)}}{w}\right)^2 r dr d\theta dx$$
$$= \frac{\mu_0\pi}{6}(N_1 I_{1(pk)})^2 \frac{od^2-id^2}{(od-id)^2} \tag{6}$$

Applying this technique to the mmf associated with the secondary winding and winding separator, summing the contributions and using (3) reveals the primary side leakage

inductance,

$$L_{lk1} = \frac{\mu_0 \pi (od+id) N_1^2}{6(od-id)} (h + 2d) \tag{7}$$

Using (7) and the equivalent circuit definitions, the magnetising inductance is defined as,

$$L_m = N_1^2 \left[A_L(AF) - \frac{\mu_0 \pi (od+id)}{6(od-id)} (h + 2d) \right] \tag{8}$$

3. Align factor (AF)

In most transformers and inductors the windings are wound over the entire height of the bobbin, and so the assumption is that the flux is uniformly distributed. With integrated magnetic components this is not necessarily the case, and so the standard expressions that are used to calculate inductance are not sufficiently accurate. The flux density plots depicted in Fig. 3 were obtained from a detailed axisymmetric finite element analysis and show the difference between a fully distributed winding consisting of 100 turns on a PC 26/16 core with l_g=1mm (Fig. 3a with L=1.46mH), and a winding covering only 19% of the bobbin height (Fig. 3b with L=1.76mH). As can be seen, with a partial height winding the flux appears to more easily leak out of the air gap and so this has the effect of increasing the inductance (by 20% in this case) and, therefore, needs to be accounted for during the design process. This section presents an alignment factor (AF) that accounts for the effects of coil winding height and its location within the winding window.
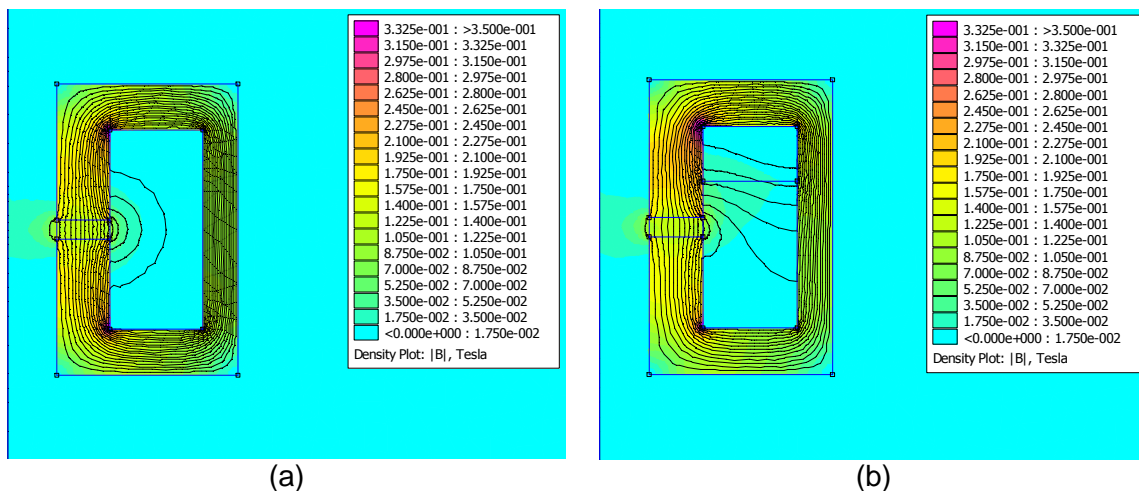
Fig. 3 Effect of winding height utilization on flux distribution, a) 100% & b) 19%

Over 1000 data points were generated using finite element analysis simulations (FEMM [6]) of pot cores inductors wound with 100 turns but featuring different airgaps and height values. The pot core dimensions (h, od, id, Ae) were taken from Magnetics Inc. Ferrites Catalogue [7]. For each core type, a specific airgap was inserted and the initial AL value measured using 100% bobbin height. Then the winding utilization was swept and the resulting AL determined. A curve-fit was performed to the data and revealed the alignment factor to be,

$$AF = 1 - 10^{-6} \sqrt{A_e} \ln\left[\frac{(h-d)^2}{4h^2}\right] / A_L \tag{9}$$

Fig. 4 shows the variation in the alignment factor value and also the inductance value for the parameters considered in the FEMM simulation sweep. As can also be seen, the effect of winding geometry can be quite significant. Fig. 4b shows the alignment factor equation predicting the inductance value with good accuracy.

(a)

(b)
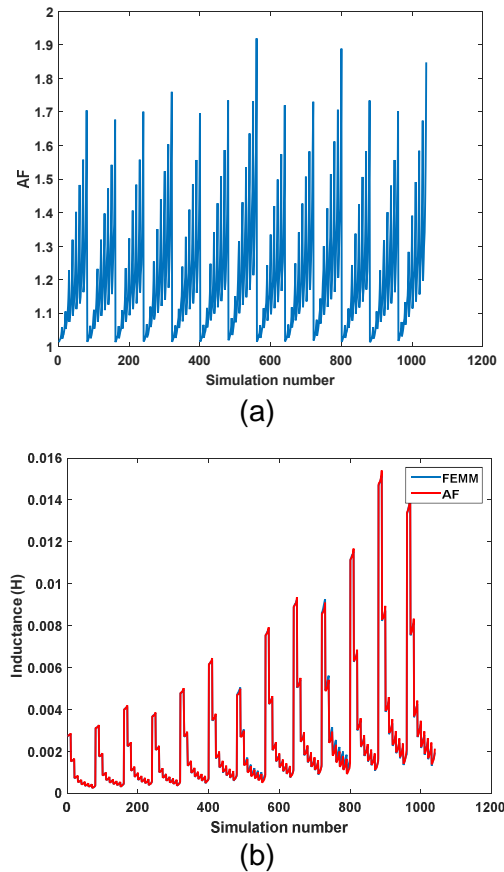
Fig. 4   Effect of winding geometry on a) alignment factor & b) inductance

4. Design procedure

The design procedure presented here allows the engineer to choose the minimum core size required to satisfy the design, whilst accounting for flux density and thermal constraints. The transformer primary voltage imposes a volt-second limitation, the high-frequency operation leads to core losses and the primary/secondary windings must be accommodated with the core winding area (W_a), and they also experience copper losses. These concerns are factored into the design process to ensure the transformer operates satisfactorily.

One needs to ensure the primary and secondary coil windings adequately fit within the winding window area W_a along with the winding separator. This leads to the following inequality where K_u ($K_u<1$) is the winding factor accounting for the actual area taken up by the winding and insulation, and J is the current density (typically 4-5 A/mm^2),

$$W_a \geq dw + \frac{1}{K_u}\left(\frac{N_1 I_{1(rms)}}{J} + \frac{N_2 I_{2(rms)}}{J}\right) \approx dw + 2\frac{N_1 I_{1(rms)}}{K_u J} \tag{10}$$

Substituting for the inductor definition $NA_eB = LI$ (where A_e is the effective core area) gives,

$$W_a \geq dw + 2\frac{L_1 I_{1(rms)} I_{1(pk)}}{K_u A_e B J} \tag{11}$$

Many ferrite material manufacturers provide detailed design information, including relationships for the limits imposed on maximum flux density level for specific operating frequency and temperature rise. Magnetics Inc., for example, provide a graphical relationship for their P type ferrite material [7] when operating with a 25°C temperature rise. A curve fit to this data (shown in Fig. 5) gives the following relationship between the *optimal* flux density (B_{opt}) and operating frequency (f) over the range 30kHz-1MHz,

$$B_{opt} = 0.0688z^2 - 0.4366z + 0.7054 \qquad (12)$$

where $z = \log(f)$ with f in kHz.
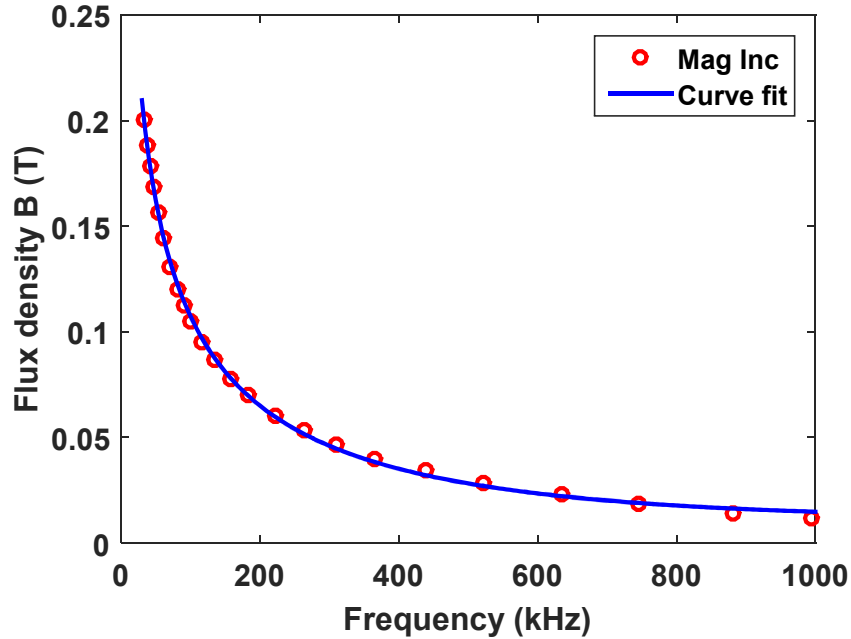
Figure 5: Curve fit to Magnetics Inc. P type ferrite material recommended operating flux density

Rearranging (11) and using (12) gives the minimum area product (AP) required to satisfy the design specification. Note, the inequality in (13) is factored to give the geometry specific relationship on the left hand side and the electrical specification on the right hand side.

$$AP = (W_a - dw)A_e \geq 2\frac{L_1 I_{1(rms)} I_{1(pk)}}{K_u B_{opt} J} \qquad (13)$$

The core inductance factor (A_L) required to ensure the core does not saturate can be found by equating the primary winding volt-second product (λ_1) to the flux density swing experienced by the winding.

$$\lambda_1 = \int_0^{T/2} |V_1(t)| dt \qquad (14)$$

During a positive half-cycle of the primary voltage, the flux density swings between its positive and negative peaks such that the peak flux density (B_{pk}) can be defined as,

$$B_{pk} = B_{opt} = \frac{\lambda_1}{2N_1 A_e} \qquad (15)$$

Thus, rearranging (1) and using (15) provides the required core specific inductance value,

$$A_L = \frac{L_{1oc}}{\left(\frac{\lambda_1}{2B_{opt} A_e}\right)^2 (AF)} \qquad (16)$$

The relationship between the effective turn ratio and actual turn ratio is given by,

$$n_e = \frac{N_1}{N_2}\sqrt{\frac{A}{A+1}} \qquad (17)$$

where $A=L_m/L_{lk1}$

The above constraints are incorporated into a design procedure as follows,

1460

1. Specify all electrical parameters for the IM and the intended winding separator distance d
2. Determine the optimum flux density (B_{opt}) at which to run the core using (12)
3. Choose the smallest core which meets the AP value in (13). This will then fix the core geometry (h, w=0.5(od-id), A_e)
4. Determine the required A_L value to achieve B_{opt} using (16)
5. Transformer winding turns should be chosen to best meet the desired turn ratio and required inductances
   a. Determine the primary turns N_1 using (1) and then use (17) to determine secondary turns N_2
   b. Or determine the secondary turns N_2 using (2) and then use (17) to determine the primary turns N_1
6. Choose appropriate wire sizes, accounting for high frequency effects as necessary, and confirm the windings fit within the winding window

Should the windings not fit within the winding window it may be necessary to:
1. Choose a larger core
2. Reduce the separation distance d
3. Operate at different flux density
4. Modify the desired inductances and/or turn ratio

5. Design example and validation

To validate the pot core integrated magnetic component design methodology a 25W, 45-55V input to 5V output LLC resonant converter was designed using the LLCDesigner software [8,9]. The specification for the integrated magnetic component is L_{lk1}=5.1µH, L_m=23.1µH, n_e=5.5 with a minimum operating frequency of f=200kHz and a peak primary current of $I_{1(pk)}$=2A. The winding separator distance was chosen as d=5mm. From (12) the optimum flux density was determined as B_{opt}~65mT. Using J=4A/mm and K_u=0.5 the minimum core area product was determined to be,

$$AP = (W_a - dw)A_e \geq 1.23 \times 10^{-9} \text{m}^4 \qquad (18)$$

With the required separator distance, a 26/16 pot core with an $AP = 2.9 \times 10^{-9}\text{m}^4$ was chosen. With an inductance ratio A=4.55, the actual turn ratio was determined to be,

$$n = \frac{N_1}{N_2} \approx 6 \qquad (19)$$

The actual number of turns on the primary winding was determined as N_1=12, giving N_2=2. Fig. 6 shows the flux density plot taken from FEMM which was used to measure the primary inductance L_1=28.35µH and mutual inductance M=3.69µH. These values were then used to determine the leakage inductance L_{lk1}=6.22µH and magnetizing inductance L_m=22.13µH, which are very close to the design. A prototype IM was built to the same design specification. Experimental measurements taken using an LCR bridge revealed the leakage inductance L_{lk1}=5.86µH, magnetizing inductance L_m=20.76µH and the effective turn ratio n_e=5.3, values which are close to the design specification.
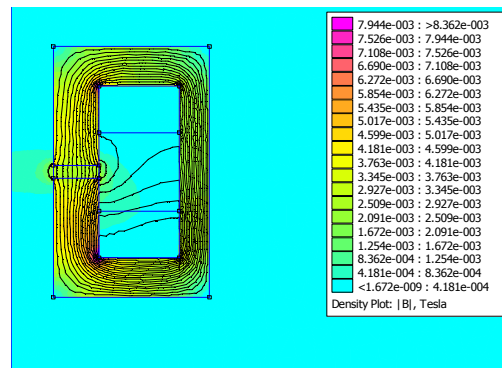
Fig. 6 Flux distribution in the design example

6. Conclusion

A model for a pot core integrated magnetic component has been developed which allows the leakage inductance, magnetizing inductance and effective turn ratio to be predicted. We have introduced an alignment factor (AF) which modifies the inductance equation to account for the additional leakage inductance caused by the non-uniformly distributed windings. A design procedure has been presented which allows the engineer to determine the minimum required core size, operating flux density, A_L factor and primary & secondary turns. A design example based on an LLC resonant converter has been given and results obtained from finite element analysis show good agreement.

Acknowledgment

References

[1] A. Kats, G. Ivensky & S. Ben-Yaakov, 'Application of integrated magnetics in resonant converters', IEEE Applied Power Electronics Conference and Exposition (APEC), pp. 925 – 930, vol.2, 1997.

[2] B. Yang, R. Chen & F. C. Lee, 'Integrated magnetic for LLC resonant converter', IEEE Applied Power Electronics Conference and Exposition (APEC), pp. 346-351, vol. 1, 2002.

[3] S. De Simone, C. Adragna, C. & C. Spini, 'Design guideline for magnetic integration in LLC resonant converters', IEEE International Symposium on Power Electronics, Electrical Drives, Automation and Motion (SPEEDAM 2008), pp. 950 – 957, 2008.

[4] S. A. El-Hamamsy & E. I. Chang, 'Magnetics modeling for computer-aided design of power electronics circuits', IEEE Power Electronics Specialists Conference (PESC), pp. 635 – 645, vol. 2, 1989.

[5] J. van Rensburg, P. A. & H. C. Ferreira, 'The role of magnetizing and leakage inductance in transformer coupling circuitry', International Symposium. Power-line Communications, pp. 244-249, 2004.

[6] D. C. Meeker, Finite Element Method Magnetics (FEMM), http://www.femm.info

[7] Magnetics Inc. Ferrite Cores 2013 Catalog.

[8] LLCDesigner, http://www.mpfoster.staff.shef.ac.uk/

[9] M. P. Foster, D. A. Stone & C. M. Bingham, An automated design methodology for LLC resonant converters using a genetic algorithm, Power Electronics, Intelligent Motion, Renewable Energy and Energy Management PCIM 2009 Europe, 2009.